

Context-Aware Doubly-Robust Semi-Supervised Learning

Clement Ruah, *Graduate Student Member, IEEE*, Housseem Sifaou, *Member, IEEE*,
 Osvaldo Simeone, *Fellow, IEEE*, and Bashir Al-Hashimi
 CIIPS, Department of Engineering, King’s College London, London, UK

Abstract—The widespread adoption of artificial intelligence (AI) in next-generation communication systems is challenged by the heterogeneity of traffic and network conditions, which call for the use of highly contextual, site-specific, data. A promising solution is to rely not only on real-world data, but also on synthetic pseudo-data generated by a network digital twin (NDT). However, the effectiveness of this approach hinges on the accuracy of the NDT, which can vary widely across different contexts. To address this problem, this paper introduces context-aware doubly-robust (CDR) learning, a novel semi-supervised scheme that adapts its reliance on the pseudo-data to the different levels of fidelity of the NDT across contexts. CDR is evaluated on the task of downlink beamforming, showing superior performance compared to previous state-of-the-art semi-supervised approaches.

Index Terms—Digital Twin, 6G, Prediction-Powered Inference, Doubly-Robust Learning

I. INTRODUCTION

We are currently in the *scaling era* of artificial intelligence (AI), where progress is largely driven by simultaneous increases in both data availability and computational resources [1]. However, this paradigm presents significant challenges for applications in engineering systems such as telecommunication networks. In fact, these systems are inherently constrained by the computational resources they can feasibly utilize from an economic standpoint, and their data are highly *contextual*. For example, the data logs for the physical layer of a telecommunication network are site- and time-specific, influenced by user location and mobility patterns, as well as by the geometry and variability of the surrounding physical environment [2].

The scarcity of data tailored to a given *context*—such as the prevailing site geometry and traffic conditions—can be mitigated through the use of *network digital twins* (NDTs) [3]–[9]. An NDT can be designed to approximate the given contextual conditions, generating *pseudo-data* that retains statistical properties similar to those of the corresponding, yet unavailable, real-world data. These pseudo-data can then be used to supplement the available real data, enhancing the training of AI models.

In this paper, we focus on a common *semi-supervised learning* framework in which the designer has access not

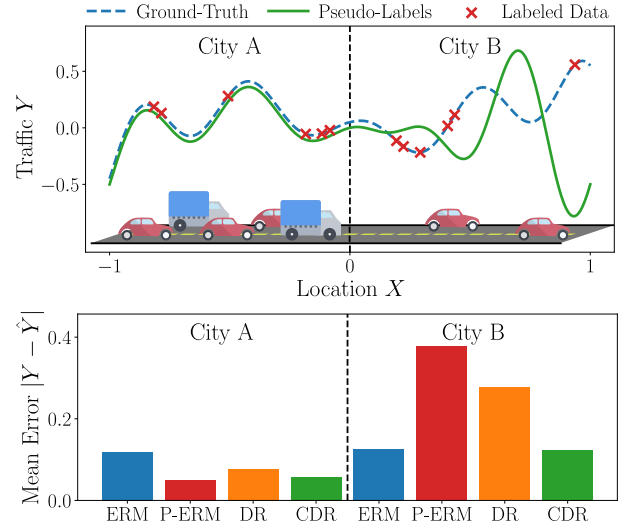


Fig. 1: (top) Toy example dataset with scalar location covariate $X \in [-1, 1]$ and deterministic target $Y \in \mathbb{R}$ representing traffic conditions. (bottom) Average error $|\hat{Y} - Y|$ per context $C \in \{\text{“City A”}, \text{“City B”}\}$ between ground-truth targets Y and predictions \hat{Y} from models trained using supervised ERM (blue), P-ERM (red), DR (orange) and CDR (green) learning.

only to labeled data but also to a pool of unlabeled data. Additionally, a *teacher model*, which can be derived from an NDT, is available to assign *pseudo-labels* to the unlabeled data. The conventional approach, referred to as *pseudo-empirical risk minimization* (P-ERM), trains a target model by minimizing the empirical loss computed over both labeled and pseudo-labeled data [10]. Consequently, the generalization performance of P-ERM is heavily dependent on the accuracy of the teacher model.

To address this limitation, reference [11] introduced *doubly-robust* (DR) self-training, a methodology inspired by [12], which corrects for the bias introduced by inaccuracies in pseudo-labels during training. However, when applied to telecommunication networks, a key shortcoming of DR is its failure to account for contextual information. In practice, the accuracy of the teacher model—such as that of an NDT—can vary significantly depending on the context. For instance, in the stylized scenario depicted in Fig. 1, the pseudo-labels exhibit high accuracy inside the context $C = \text{“City A”}$ while they are significantly less reliable at locations within context

C. Ruah, H. Sifaou, and O. Simeone are with King’s Communications, Learning & Information Processing (KCLIP) Lab. The work of C. Ruah was supported by the Faculty of Natural, Mathematical, and Engineering Sciences at King’s College London. The work of H. Sifaou and O. Simeone was partially supported by the European Union’s Horizon Europe project CENTRIC (101096379). O. Simeone was also supported by the Open Fellowships of the EPSRC (EP/W024101/1) and by the EPSRC project (EP/X011852/1).

$C = \text{“City B”}$. When contextual information is available, an ideal training strategy should incorporate pseudo-labels in a manner that dynamically adjusts based on their reliability across different contexts.

In this work, we introduce *context-aware doubly-robust* (CDR) learning, an extension of DR that adaptively adjusts the weighting of pseudo-labeled samples based on contextual information. As demonstrated in the toy example in Fig. 1, CDR effectively compensates for context-dependent errors in pseudo-labels, outperforming all existing state-of-the-art methods.

II. PROBLEM DEFINITION

We consider a learning setting involving not only covariates $X \in \mathcal{X}$ and target variables, or labels, $Y \in \mathcal{Y}$, but also discrete *context* variables $C \in \{1, \dots, K\}$ associated to each pair (X, Y) . The context variable C *stratifies* the input-output pairs (X, Y) into $K \geq 1$ separate categories, representing properties shared by multiple data points. These include, e.g., anagraphical features like age, or aspects associated with data collection, like location.

We focus on a *semi-supervised* learning problem formulation characterized by a *labeled dataset* $\mathcal{D} = \{(x_i, c_i, y_i)\}_{i=1}^n \stackrel{\text{i.i.d.}}{\sim} P(X, C, Y)$, and an *unlabeled dataset* $\tilde{\mathcal{D}} = \{(\tilde{x}_i, \tilde{c}_i)\}_{i=1}^N \stackrel{\text{i.i.d.}}{\sim} P(X, C)$. Both datasets consist of independent and identically distributed (i.i.d.) variables that follow the same population distribution $P(X, C, Y) = P(C)P(X|C)P(Y|X, C)$. In addition to the datasets, learning can leverage a pre-trained *teacher model* $f : \mathcal{X} \rightarrow \mathcal{Y}$ that assigns an estimate $f(X)$ of the target variable $Y \in \mathcal{Y}$ associated to covariate $X \in \mathcal{X}$ [11], [13]. Leveraging the datasets \mathcal{D} and $\tilde{\mathcal{D}}$, as well as the teacher model f , the goal is to train a parametric probabilistic model $p(y|x, \theta)$ by optimizing over the parameter vector $\theta \in \Theta$. For a given loss function $\ell(\theta|x, y)$, the optimality of the trained parameter $\hat{\theta}$ is evaluated through the corresponding *population loss* $\mathcal{L}(\hat{\theta}) = \mathbb{E}_{X, Y \sim P(X, Y)}[\ell(\hat{\theta}|X, Y)]$. In what follows, we will use the notation

$$L_{\ell, \mathcal{D}}(\theta) = \frac{1}{|\mathcal{D}|} \sum_{(x, y) \in \mathcal{D}} \ell(\theta|x, y) \quad (1)$$

for the empirical loss evaluated on a given dataset \mathcal{D} and loss function $\ell(\theta|x, y)$.

III. STATE OF THE ART

State-of-the-art methods do not account for contextual information. In particular, the standard approach to address the semi-supervised learning problem outlined in the previous section is to augment the labeled dataset \mathcal{D} with the synthetic labeled dataset $\tilde{\mathcal{D}}^f = \{(\tilde{x}_i, f(\tilde{x}_i))\}_{i=1}^N$, in which the labels are imputed using the teacher model f , obtaining the *pseudo-labels* $\{f(\tilde{x}_i)\}_{i=1}^N$ [13]. This leads to a training objective of the form

$$L^{\text{P-ERM}}(\theta) = L_{\ell, \mathcal{D} \cup \tilde{\mathcal{D}}^f}(\theta) \quad (2)$$

whose optimization is referred as *pseudo-empirical risk minimization* (P-ERM). The P-ERM training objective

$L^{\text{P-ERM}}(\theta)$ in (2) is a biased estimate of the population loss $\mathcal{L}(\theta)$, leading to an inconsistent estimate $\hat{\theta}^{\text{P-ERM}} = \arg \min_{\theta \in \Theta} L^{\text{P-ERM}}(\theta)$ of the population loss minimizer $\theta^* = \arg \min_{\theta \in \Theta} \mathcal{L}(\theta)$ [14, Ch. 5].

In order to circumvent this drawback, the *doubly-robust* (DR) scheme introduced in [11] adopts the training objective

$$L^{\text{DR}}(\theta) = L_{\ell, \mathcal{D}^f \cup \tilde{\mathcal{D}}^f}(\theta) - \underbrace{(L_{\ell, \mathcal{D}^f}(\theta) - L_{\ell, \mathcal{D}}(\theta))}_{\text{bias correction}}, \quad (3)$$

where the dataset $\mathcal{D}^f = \{(x_i, f(x_i))\}_{i=1}^n$ replaces the available targets $\{y_i\}_{i=1}^n$ with their corresponding pseudo-labels $\{f(x_i)\}_{i=1}^n$. In (3), the first term $L_{\ell, \mathcal{D}^f \cup \tilde{\mathcal{D}}^f}(\theta)$ is the empirical loss based solely on pseudo-labels, while the second term corrects for the bias caused by the use of the teacher model. This leads to an unbiased estimate of the population loss, i.e., $\mathbb{E}[L^{\text{DR}}(\theta)] = \mathcal{L}(\theta)$, and to a consistent estimate $\hat{\theta}^{\text{DR}} = \arg \min_{\theta \in \Theta} L^{\text{DR}}(\theta)$ of the population loss minimizer θ^* .

IV. CONTEXT-AWARE DOUBLY-ROBUST SELF-TRAINING

In this section, we introduce *context-aware doubly-robust* (CDR) semi-supervised learning, a novel context-aware generalization of the DR training method presented in the previous section.

A. Context-Aware Doubly-Robust Training Objective

CDR starts by partitioning the labeled and unlabeled datasets as $\mathcal{D}_c = \{(x_i^c, y_i^c)\}_{i=1}^{n_c} = \{(x_i, y_i) | 1 \leq i \leq n, c_i = c\}$ and $\tilde{\mathcal{D}}_c = \{\tilde{x}_i^c\}_{i=1}^{N_c} = \{\tilde{x}_i | 1 \leq i \leq N, \tilde{c}_i = c\}$, respectively, for each value $c \in \{1, \dots, K\}$ of the context variable C . The datasets \mathcal{D}^f and $\tilde{\mathcal{D}}^f$ including the pseudo-labels are similarly partitioned as $\mathcal{D}_c^f = \{(x_i^c, f(x_i^c))\}_{i=1}^{n_c}$ and $\tilde{\mathcal{D}}_c^f = \{(\tilde{x}_i^c, f(\tilde{x}_i^c))\}_{i=1}^{N_c}$ for $c \in \{1, \dots, K\}$. With these stratified datasets, the CDR objective generalizes the DR training loss in (3) by breaking down the contributions of the labeled and unlabeled data across the values of the context variable C and introducing a tuning parameter $\lambda_c \in [0, 1]$ for each context value c . This yields the criterion

$$L_{\ell}^{\text{CDR}(\lambda)}(\theta) = \sum_{c=1}^K \left\{ \frac{\lambda_c N_c}{N} L_{\ell, \tilde{\mathcal{D}}_c^f}(\theta) + \left(\frac{n_c}{n} L_{\ell, \mathcal{D}_c}(\theta) - \frac{\lambda_c n_c}{n} L_{\ell, \mathcal{D}_c^f}(\theta) \right) \right\}, \quad (4)$$

where $\lambda = [\lambda_1, \dots, \lambda_K] \in [0, 1]^K$ is a *tuning parameter vector*.

The inclusion of the parameters λ_c in (4) allows CDR to account for the extent to which the trained model relies on the pseudo-labeled data $\tilde{\mathcal{D}}_c^f$ at context c . Specifically, setting $\lambda_c = 0$ forces CDR not to use the pseudo-labels for context c , while larger values of λ_c ensure the use of the pseudo-labels for context c in the estimate (4) [15]. Note that the DR objective in (3) is recovered as a special case of the CDR objective $L_{\ell}^{\text{CDR}(\lambda)}(\theta)$ when all entries of λ are set $\lambda_c = 1/(1 + n/N)$. By varying the tuning parameter λ_c with the context c , CDR gains the flexibility to adjust the estimate (4) to different levels of accuracy of the teacher model, while maintaining unbiasedness, i.e., the equality $\mathbb{E}[L_{\ell}^{\text{CDR}(\lambda)}(\theta)] = \mathcal{L}(\theta)$, regardless of the value of λ .

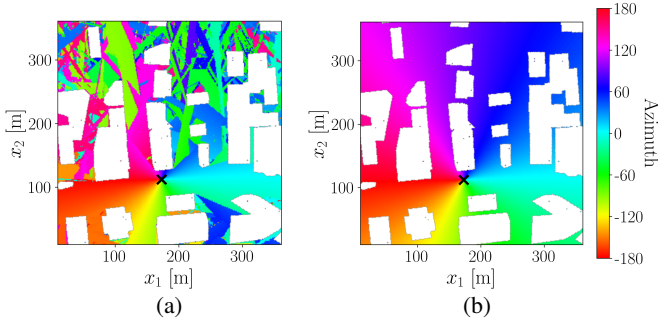


Fig. 2: Horizontal slice of the map of the urban region of interest in the beamforming experiments of Sec. V. The layouts of the buildings are depicted as empty white regions, and the BS position is marked by a black cross. The colored regions in (a) depict the ground-truth azimuth angles of the strongest path at each device location, while (b) reports the teacher model's azimuth estimates, which ignore the presence of LoS blockages due to buildings.

B. Optimal Tuning Parameter

CDR addresses the minimization of the objective (4) using gradient descent (GD). Accordingly, at each iteration t , CDR tackles the problem

$$\hat{\theta}_{t+1} = \arg \min_{\theta \in \Theta} L_{\ell_t}^{\text{CDR}(\lambda_t)}(\theta), \quad (5)$$

where $\ell_t(\theta|x, y)$ is the local quadratic approximation of the loss function $\ell(\theta|x, y)$ around the current iterate $\hat{\theta}_t$. This is given by

$$\ell(\hat{\theta}_t|x, y) + \nabla_{\theta} \ell(\hat{\theta}_t|x, y)^{\top} (\theta - \hat{\theta}_t) + \frac{1}{2\gamma_t} \|\theta - \hat{\theta}_t\|^2, \quad (6)$$

where $\gamma_t > 0$ is the learning rate [16]. The tuning vector $\lambda_t = [\lambda_{t,1}, \dots, \lambda_{t,K}]$ is chosen at each time t to minimize the variance of the next parameter estimate $\hat{\theta}_{t+1}$ in (5). Following [17, Prop. 2], the ideal solution to this problem is obtained as

$$\lambda_{t,c}^* = \frac{\mathbb{E}_c \left[(\nabla \ell^f - \nabla \mathcal{L}_c^f)^{\top} (\nabla \ell - \nabla \mathcal{L}_c) \right]}{\left(1 + \frac{n_c}{N_c} \right) \mathbb{E}_c \left[\left\| \nabla \ell^f - \nabla \mathcal{L}_c^f \right\|^2 \right]}, \quad (7)$$

for $c \in \{1, \dots, K\}$, where $\mathbb{E}_c[\cdot]$ is a shorthand for the context-dependent average $\mathbb{E}_{X,Y \sim P(X,Y|C=c)}[\cdot]$, and $\nabla \ell = \nabla_{\theta} \ell(\theta_t|X, Y)$ and $\nabla \ell^f = \nabla_{\theta} \ell(\theta_t|X, f(X))$ are the gradient and pseudo-gradient vectors at the current iterate θ_t , with respective means $\nabla \mathcal{L}_c = \mathbb{E}_c[\nabla \ell]$ and $\nabla \mathcal{L}_c^f = \mathbb{E}_c[\nabla \ell^f]$. Intuitively, the optimal parameter $\lambda_{t,c}^*$ measures the level of agreement between the centered gradients $(\nabla \ell - \nabla \mathcal{L}_c)$ and centered pseudo-gradients $(\nabla \ell^f - \nabla \mathcal{L}_c^f)$ within context c via an averaged cosine similarity. The ideal solution $\lambda_{t,c}^*$, however, depends on the true data distribution, which is unknown. Therefore, CDR estimates the expected values in (7) using the labeled data \mathcal{D}_c as in [17]. Accordingly, the only additional complexity of CDR as compared to DR is the evaluation of the vector λ_t^* with entries (7).

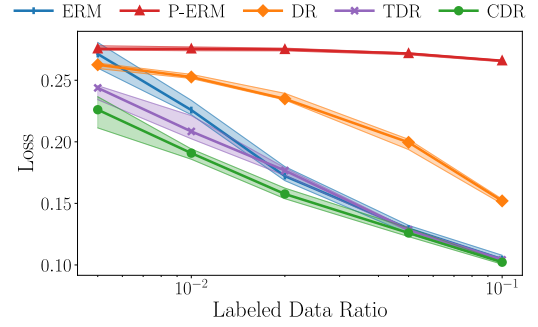


Fig. 3: Test loss as a function of the labeled data ratio ρ for ERM, P-ERM (2), DR [11], TDR, and the proposed CDR (4). The solid lines represent the median of 10 independent runs, and shaded areas indicate the range between the first and the third quartiles.

V. EXPERIMENTS

In this section, we study self-training for position-based downlink beamforming [18], [19]. The code used to carry the experiments is available at [20].

Setup: As depicted in Fig. 2, we consider an outdoor urban setting with a single base station (BS), where propagation paths between the BS and the devices are generated using ray-tracing as in [18]. As seen in Fig. 2a for the azimuth, each device position $X \in \mathbb{R}^3$ is associated with a ground-truth optimal azimuth and elevation angle of departure (AoD) $Y = (Y^{\text{az}}, Y^{\text{el}}) \in \mathcal{A} = [-\pi, \pi) \times [0, \pi]$ obtained by considering the propagation path with the highest received power. Positions X on the three dimensional space are uniformly sampled on the regions of the horizontal slice depicted in Fig. 2 that are not occupied by buildings. The objective is to train a mapping $g_{\theta} : \mathbb{R}^3 \rightarrow \mathcal{A}$ that outputs an estimate of the optimal AoD at each device location.

We produce a labeled training dataset of $N^{\text{tr}} = 30000$ training pairs $\mathcal{D}^{\text{tr}} = \{(x_i^{\text{tr}}, y_i^{\text{tr}})\}_{i=1}^{N^{\text{tr}}}$ and a labeled test dataset of $N^{\text{te}} = 5975$ test pairs $\mathcal{D}^{\text{te}} = \{(x_i^{\text{te}}, y_i^{\text{te}})\}_{i=1}^{N^{\text{te}}}$. Furthermore, we augment each data point with a binary context variable $c_i \in \{0, 1\}$, where $c_i = 1$ indicates that the device at location x_i is within *line of sight* (LoS) of the BS, and we set $c_i = 0$ otherwise, i.e., for *non-line of sight* (NLoS) coordinates. The training dataset $\{(x_i^{\text{tr}}, c_i^{\text{tr}}, y_i^{\text{tr}})\}_{i=1}^{N^{\text{tr}}}$ is randomly split into $n = \lceil \rho N^{\text{tr}} \rceil$ labeled samples $\mathcal{D} = \{(x_i, c_i, y_i)\}_{i=1}^n$ and $N = N^{\text{tr}} - n$ unlabeled samples $\tilde{\mathcal{D}} = \{(\tilde{x}_i, \tilde{c}_i)\}_{i=1}^N$, where the labeled data ratio $\rho \in [0, 1]$ varies from 0.5% to 10%.

The teacher model $f(x)$ disregards the geometry of the scene, producing pseudo-labels equal to the azimuth and elevation angles of the LoS propagation path connecting the BS and the device at location x . As a result, as depicted in Fig 2b for the azimuth, the teacher model is equal to the target angles in LoS regions ($c = 1$), while presenting large discrepancies with the ground-truth target angles for NLoS conditions ($c = 0$).

Implementation: As in [21], the trainable map g_{θ} is implemented as a feedforward neural network with an initial Fourier feature layer and two hidden layers with parameters θ . Writing the model's output as $g_{\theta}(x) = (\hat{y}^{\text{az}}, \hat{y}^{\text{el}}) \in \mathcal{A}$, the loss function is defined as the sum $\ell_{\theta}(x, y) = h(\hat{y}^{\text{az}}, y^{\text{az}}) + h(\hat{y}^{\text{el}}, y^{\text{el}})$,

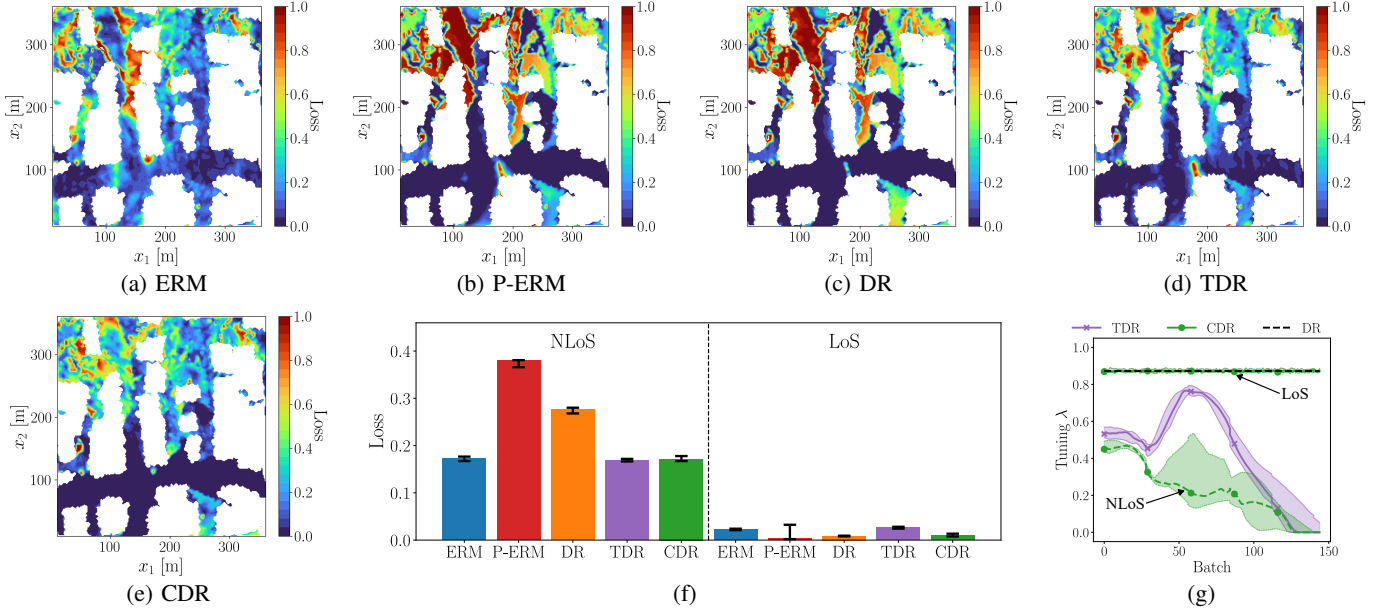


Fig. 4: Test loss maps for the (a) ERM, (b) P-ERM (2), (c) DR [11], (d) TDR, and (e) CDR (4) with $n = 150$ labeled data points. (f) Test loss per context. (g) Evolution of the computed tuning parameters λ through training for TDR (purple) and CDR in NLoS (green dashed) and LoS (green solid) conditions, as well as the effective tuning parameter $1/(1+n/N)$ assumed by DR (black dashed). All levels correspond to the median of 10 independent runs, and error bars in (f) and shaded areas in (g) indicate the range between the first and the third quartiles.

where $y = (y^{\text{az}}, y^{\text{el}})$ is the ground-truth target associated to position x , and $h(\hat{\varphi}, \varphi) = 1 - \cos(\hat{\varphi} - \varphi)$ is the log-loss for a von Mises model with independent azimuth and elevation angles with respective means \hat{y}^{az} and \hat{y}^{el} [22].

Benchmarks: Apart from the P-ERM and DR self-training procedures introduced in Sec. III, we also consider the following benchmarks: 1) *empirical risk minimization* (ERM), which minimizes the standard loss $L_{\ell, \mathcal{D}}(\theta)$ limited to the labeled data; and 2) *tuned doubly-robust* (TDR) learning, which addresses the CDR objective (4) with $\lambda_c = \lambda_0 \in [0, 1]$ for all contexts $c \in \{1, \dots, K\}$, thus ignoring contextual information.

DR is implemented by adopting the curriculum-based time-varying loss proposed in the original paper [11], and a similar implementation is also used for TDR and CDR schemes, minimizing a time-varying loss of the form

$$L_{\ell, \alpha_e}^{\text{CDR}(\lambda)}(\theta) = \sum_{c=1}^K \left\{ \frac{\lambda_c N_c}{N} L_{\ell, \mathcal{D}_c^f}(\theta) + \alpha_e \left(\frac{n_c}{n} L_{\ell, \mathcal{D}_c}(\theta) - \frac{\lambda_c n_c}{n} L_{\ell, \mathcal{D}_c^f}(\theta) \right) \right\}, \quad (8)$$

with the linear schedule $\alpha_e = e/E$ over the total number of epochs E .

Results: Fig. 3 presents the test loss $L_{\ell, \mathcal{D}^{\text{te}}}(\hat{\theta})$ for the estimates $\hat{\theta}$ described above as a function of the labeled data ratio. Given that P-ERM and DR do not have any mechanism to account for the accuracy of the teacher model f , they achieve a test loss larger than ERM, which neglects pseudo-labeled data. In contrast, by selectively trusting the teacher model f depending on the LoS/NLoS context, the proposed CDR outperforms

all baselines, especially in the more challenging regime with limited labeled data.

The variability of the test loss $\ell(\hat{\theta}|X, Y)$ as a function of the location X is displayed on a two-dimensional map in Fig. 4a-4e for $\rho = 0.005$, i.e., for $n = 150$ labeled samples. As emphasized in Fig 4f, P-ERM and DR display near optimal performance in LoS regions, where the teacher model f is accurate, but they are outperformed by ERM in NLoS areas, where the teacher model f is unreliable. In contrast, TDR closely aligns with ERM, since, as shown in Fig. 4g, the learned tuning parameter λ_0 converges to 0 during training to accommodate the inaccuracies of f on NLoS regions. In comparison, as also shown in Fig. 4g, the proposed CDR scheme is able to account for the different accuracy levels of the teacher f in LoS and NLoS conditions, matching the performance of DR in LoS locations and of ERM in NLoS areas.

VI. CONCLUSION

This work has proposed a novel CDR semi-supervised learning scheme that adapts the importance of synthetically labeled samples to the accuracy of the teacher model at each given context via a tuning parameter vector. An optimal choice of tuning parameter was derived as a function of the similarity between ground-truth and synthetically generated gradients. Experiments on downlink beamforming empirically validated the advantage of CDR over context-agnostic P-ERM and DR self-training methodologies. Future work may investigate the adaptation of CDR to other successive convex approximation schemes [23]–[25]; or the extension to continuous context variables using kernel methods [26].

REFERENCES

- [1] L. Xiao, "Rethinking conventional wisdom in machine learning: From generalization to scaling," *arXiv preprint arXiv:2409.15156*, 2024.
- [2] F. Kaltenberger, T. Melodia, I. Ghauri, M. Polese, R. Knopp, T. T. Nguyen, S. Velumani, D. Villa, L. Bonati, R. Schmidt *et al.*, "Driving innovation in 6G wireless technologies: The OpenAirInterface approach," *arXiv preprint arXiv:2412.13295*, 2024.
- [3] L. U. Khan, W. Saad, D. Niyato, Z. Han, and C. S. Hong, "Digital-twin-enabled 6G: Vision, architectural trends, and future directions," *IEEE Communications Magazine*, vol. 60, no. 1, pp. 74–80, 2022.
- [4] S. Jiang and A. Alkhateeb, "Digital twin based beam prediction: Can we train in the digital world and deploy in reality?" *arXiv preprint arXiv:2301.07682*, 2023.
- [5] C. Ruah, O. Simeone, J. Hoydis, and B. Al-Hashimi, "Calibrating wireless ray tracing for digital twinning using local phase error estimates," *IEEE Transactions on Machine Learning in Communications and Networking*, 2024.
- [6] M. S. Abouamer, R. J. Williams, and P. Popovski, "Geometry-informed channel statistics prediction based upon uncalibrated digital twins," *arXiv preprint arXiv:2411.13360*, 2024.
- [7] J. Chen, S. Park, P. Popovski, H. V. Poor, and O. Simeone, "Neuromorphic split computing with wake-up radios: Architecture and design via digital twinning," *arXiv preprint arXiv:2404.01815*, 2024.
- [8] H. Sifaou and O. Simeone, "Semi-supervised learning via cross-prediction-powered inference for wireless systems," *arXiv preprint arXiv:2405.15415*, 2024.
- [9] Q. Hou, M. Zecchin, S. Park, Y. Cai, G. Yu, K. Chowdhury, and O. Simeone, "Automatic AI model selection for wireless systems: Online learning via digital twinning," *IEEE Transactions on Wireless Communications*, 2025.
- [10] R. Jiao, Y. Zhang, L. Ding, B. Xue, J. Zhang, R. Cai, and C. Jin, "Learning with limited annotations: a survey on deep semi-supervised learning for medical image segmentation," *Computers in Biology and Medicine*, vol. 169, p. 107840, 2024.
- [11] B. Zhu, M. Ding, P. Jacobson, M. Wu, W. Zhan, M. Jordan, and J. Jiao, "Doubly-robust self-training," *Advances in Neural Information Processing Systems*, vol. 36, 2024.
- [12] A. N. Angelopoulos, S. Bates, C. Fannjiang, M. I. Jordan, and T. Zrnica, "Prediction-powered inference," *Science*, vol. 382, no. 6671, pp. 669–674, 2023.
- [13] M.-R. Amini, V. Feofanov, L. Pautetto, L. Hadjadj, E. Devijver, and Y. Maximov, "Self-training: A survey," *Neurocomputing*, vol. 616, p. 128904, 2025.
- [14] A. W. Van der Vaart, *Asymptotic statistics*. Cambridge university press, 2000, vol. 3.
- [15] A. N. Angelopoulos, J. C. Duchi, and T. Zrnica, "PPI++: Efficient prediction-powered inference," *arXiv preprint arXiv:2311.01453*, 2023.
- [16] O. Simeone, *Machine Learning for Engineers*. Cambridge University Press, 2022.
- [17] A. Fisch, J. Maynez, R. A. Hofer, B. Dhingra, A. Globerson, and W. W. Cohen, "Stratified prediction-powered inference for hybrid language model evaluation," *arXiv preprint arXiv:2406.04291*, 2024.
- [18] Y. Zeng and X. Xu, "Toward environment-aware 6G communications via channel knowledge map," *IEEE Wireless Communications*, vol. 28, no. 3, pp. 84–91, 2021.
- [19] D. Wu, Y. Zeng, S. Jin, and R. Zhang, "Environment-aware and training-free beam alignment for mmWave massive MIMO via channel knowledge map," in *2021 IEEE International Conference on Communications Workshops (ICC Workshops)*. IEEE, 2021, pp. 1–7.
- [20] C. Ruah, "Code Repository for Context-Aware Doubly-Robust Semi-Supervised Learning," 2025, online: <https://github.com/kclip/cdr-ssl>.
- [21] M. Tancik, P. Srinivasan, B. Mildenhall, S. Fridovich-Keil, N. Raghavan, U. Singhal, R. Ramamoorthi, J. Barron, and R. Ng, "Fourier features let networks learn high frequency functions in low dimensional domains," *Advances in Neural Information Processing Systems*, vol. 33, pp. 7537–7547, 2020.
- [22] K. V. Mardia and P. E. Jupp, *Directional statistics*. Wiley Online Library, 2000, vol. 2.
- [23] B. R. Marks and G. P. Wright, "A general inner approximation algorithm for nonconvex mathematical programs," *Operations research*, vol. 26, no. 4, pp. 681–683, 1978.
- [24] M. Razaviyayn, M. Hong, Z.-Q. Luo, and J.-S. Pang, "Parallel successive convex approximation for nonsmooth nonconvex optimization," *Advances in neural information processing systems*, vol. 27, 2014.
- [25] A. Liu, V. K. Lau, and B. Kananian, "Stochastic successive convex approximation for non-convex constrained stochastic optimization," *IEEE Transactions on Signal Processing*, vol. 67, no. 16, pp. 4189–4203, 2019.
- [26] T. Hofmann, B. Schölkopf, and A. J. Smola, "Kernel methods in machine learning," *The Annals of Statistics*, pp. 1171–1220, 2008.

APPENDIX A
OPTIMAL TUNING FOR LOCAL CONVEX LOSS
APPROXIMATION

In this appendix, we detail the derivation of the optimal tuning parameter presented in Sec. IV-B, starting from the more general case of an arbitrary choice of local convex approximation. To avoid notational clutter, we use $\mathbb{E}_c[\cdot]$ and $\text{Cov}_c[\cdot]$ as shorthands for $\mathbb{E}_{X,Y \sim P(X,Y|C=c)}[\cdot]$ and $\text{Cov}_{X,Y \sim P(X,Y|C=c)}[\cdot]$.

A. General Setting

Denoting as $\ell_t(\theta|X, Y)$ a local convex approximation of the loss function around the current parameter iterate θ_t , the choice of tuning parameter $\lambda_t^* = [\lambda_{t,1}^*, \dots, \lambda_{t,K}^*]$ that minimizes the asymptotic variance of the next parameter estimate $\hat{\theta}_{t+1} = \arg \min_{\theta \in \Theta} L_{\ell_t}^{\text{CDR}(\lambda_t)}(\theta)$ is obtained as a direct application of optimal power tuning in stratified prediction-powered inference (PPI) [17, Prop. 2]. Accordingly, we have

$$\lambda_{t,c}^* = \frac{\text{tr}_{\bar{H}_t} \left(C_{t,c}(\theta_{t+1}) + C_{t,c}(\theta_{t+1})^\top \right)}{2 \left(1 + \frac{n_c}{N_c} \right) \text{tr}_{\bar{H}_t} \left(V_{t,c}^f(\theta_{t+1}) \right)}, \quad (9)$$

with

$$\text{tr}_{\bar{H}_t}(A) = \text{tr} \left(\bar{H}_t(\theta_{t+1})^{-1} A \bar{H}_t(\theta_{t+1})^{-1} \right) \quad (10)$$

for an input matrix A , where $\theta_{t+1} = \arg \min_{\theta \in \Theta} \mathbb{E}_{X,Y \sim P(X,Y)}[\ell_t(\theta|X, Y)]$ is the optimal next parameter iterate;

$$V_{t,c}^f(\theta) = \text{Cov}_c[\nabla_{\theta} \ell_t(\theta|X, f(X))] \quad (11)$$

is the pseudo-loss gradient covariance;

$$C_{t,c}(\theta) = \text{Cov}_c[\nabla_{\theta} \ell_t(\theta|X, Y), \nabla_{\theta} \ell_t(\theta|X, f(X))] \quad (12)$$

is the loss and pseudo-loss gradients cross-covariance; and $\bar{H}_t(\theta) = \mathbb{E}_{C \sim P(C)}[H_{t,C}(\theta)]$ is the average of the per-context Hessians

$$H_{t,c}(\theta) = \mathbb{E}_c[\nabla_{\theta}^2 \ell_t(\theta|X, Y)]. \quad (13)$$

B. Gradient Descent Quadratic Approximation

We now simplify the optimal tuning formula in (9) for the case of GD optimization, which is implemented using a quadratic local approximation of the form

$$\begin{aligned} \ell_t(\theta|x, y) = \\ \ell(\theta_t|x, y) + \nabla_{\theta} \ell(\theta_t|x, y)^\top (\theta - \theta_t) + \frac{1}{2\gamma_t} \|\theta - \theta_t\|^2, \end{aligned} \quad (14)$$

where $\gamma_t > 0$ is the learning rate, and where $\|\cdot\|$ denotes the Euclidean norm.

We define as $\nabla \ell = \nabla_{\theta} \ell(\theta_t|X, Y)$ and $\nabla \ell^f = \nabla_{\theta} \ell(\theta_t|X, f(X))$ the gradient and pseudo-gradient vectors at the current parameter estimate θ_t , and denote their global and context-dependent means as $\nabla \mathcal{L} = \mathbb{E}_{X,Y \sim P(X,Y)}[\nabla \ell]$,

$\nabla \mathcal{L}_c = \mathbb{E}_c[\nabla \ell]$, and $\nabla \mathcal{L}_c^f = \mathbb{E}_c[\nabla \ell^f]$. From the GD local approximation (14), we have

$$\begin{aligned} \theta_{t+1} &= \theta_t - \gamma_t \nabla \mathcal{L} \\ \nabla_{\theta} \ell_t(\theta_{t+1}|X, Y) &= \nabla \ell - \nabla \mathcal{L} \\ \bar{H}_t(\theta_{t+1}) &= \gamma_t I \\ \mathbb{E}_c[\nabla_{\theta} \ell_t(\theta_{t+1}|X, Y)] &= \nabla \mathcal{L}_c - \nabla \mathcal{L} \\ \mathbb{E}_c[\nabla_{\theta} \ell_t(\theta_{t+1}|X, f(X))] &= \nabla \mathcal{L}_c^f - \nabla \mathcal{L}, \end{aligned} \quad (15)$$

where I denotes the identity matrix. Accordingly, the cross-covariance term in (9) can be expressed as

$$C_{t,c}(\theta_{t+1}) = \mathbb{E}_c \left[(\nabla \ell - \nabla \mathcal{L}_c) (\nabla \ell^f - \nabla \mathcal{L}_c^f)^\top \right]. \quad (16)$$

Using the invariance of the trace operator to cyclic permutations, we can compute the denominator in (9) as

$$\begin{aligned} \text{tr}_{\bar{H}_t}(C_{t,c}(\theta_{t+1})) \\ = \gamma_t^2 \mathbb{E}_c \left[\text{tr} \left((\nabla \ell - \nabla \mathcal{L}_c) (\nabla \ell^f - \nabla \mathcal{L}_c^f)^\top \right) \right] \\ = \gamma_t^2 \mathbb{E}_c \left[(\nabla \ell^f - \nabla \mathcal{L}_c^f)^\top (\nabla \ell - \nabla \mathcal{L}_c) \right]. \end{aligned} \quad (17)$$

Similarly, we have

$$\begin{aligned} \text{tr}_{\bar{H}_t}(V_{t,c}^f(\theta_{t+1})) = \\ \gamma_t^2 \mathbb{E}_c \left[(\nabla \ell^f - \nabla \mathcal{L}_c^f)^\top (\nabla \ell^f - \nabla \mathcal{L}_c^f) \right]. \end{aligned} \quad (18)$$

All in all, the optimal tuning parameter for gradient descent can be expressed as

$$\lambda_{t,c}^* = \frac{\mathbb{E}_c \left[(\nabla \ell^f - \nabla \mathcal{L}_c^f)^\top (\nabla \ell - \nabla \mathcal{L}_c) \right]}{\left(1 + \frac{n_c}{N_c} \right) \mathbb{E}_c \left[\left\| \nabla \ell^f - \nabla \mathcal{L}_c^f \right\|^2 \right]}. \quad (19)$$

Since the ideal solution $\lambda_{t,c}^*$ depends on the unknown data distribution $P(X, Y|C = c)$, it is instead estimated using the labeled data \mathcal{D}_c as

$$\begin{aligned} \hat{\lambda}_{t,c} = \\ \frac{\frac{1}{n_c-1} \sum_{i=1}^{n_c} \left(\nabla \ell_{c,i}^f - \nabla \hat{\mathcal{L}}_c^f \right)^\top \left(\nabla \ell_{c,i} - \nabla \hat{\mathcal{L}}_c \right)}{\left(1 + \frac{n_c}{N_c} \right) \frac{1}{n_c-1} \sum_{i=1}^{n_c} \left\| \nabla \ell_{c,i}^f - \nabla \hat{\mathcal{L}}_c^f \right\|^2}, \end{aligned} \quad (20)$$

where $\nabla \ell_{c,i} = \nabla_{\theta} \ell(\theta_t|x_i^c, y_i^c)$, $\nabla \ell_{c,i}^f = \nabla_{\theta} \ell(\theta_t|x_i^c, f(x_i^c))$, $\nabla \hat{\mathcal{L}}_c = \frac{1}{n_c} \sum_{i=1}^{n_c} \nabla \ell_{c,i}$, and $\nabla \hat{\mathcal{L}}_c^f = \frac{1}{n_c} \sum_{i=1}^{n_c} \nabla \ell_{c,i}^f$.